

# We are IntechOpen, the world's leading publisher of Open Access books Built by scientists, for scientists

6,100

Open access books available

149,000

International authors and editors

185M

Downloads

Our authors are among the

154

Countries delivered to

TOP 1%

most cited scientists

12.2%

Contributors from top 500 universities



WEB OF SCIENCE™

Selection of our books indexed in the Book Citation Index  
in Web of Science™ Core Collection (BKCI)

Interested in publishing with us?  
Contact [book.department@intechopen.com](mailto:book.department@intechopen.com)

Numbers displayed above are based on latest data collected.  
For more information visit [www.intechopen.com](http://www.intechopen.com)



## Chapter

# Analysis of the Effects Produced by Pure Sine and Modified Sine Inverters in an Induction Motor

*Arturo Yosimar Jaen-Cuellar, David Alejandro Elvira-Ortiz, Emmanuel Resediz-Ochoa and Juan Jose Saucedo-Dorantes*

## Abstract

Most of the industrial applications are supported by complex machinery, which in turn are supported by electrical motors to perform specific tasks in multiple processes. Certainly, induction motors are the most widely used electrical machines in a majority of industrial machineries; in this sense, their operating condition plays an important role to ensure the machinery availability and to avoid unwanted stoppages. On the other hand, several sources may lead to producing faults in induction motors, but most of the common faults are produced by electrical or mechanical stresses, where the mechanical stresses are usually produced by unbalances or misalignments and the electrical stresses are generated by fluctuations or variations in the power supply. Thereby, when the induction motors are fed through inverters due to renewable energy, their operation may present slight variations since the sine wave has no perfect generation. In this regard, this work presents an analysis of the effects produced by pure sine and modified sine inverters in an induction motor. Such analysis consists of studying the characteristic patterns, reflected as percentage variations in some metrics, such as ranges, rms values, and harmonic distortion, that induction motors produce over vibration signals, electrical signals (stator current and fed voltages), and rotating speed.

**Keywords:** condition monitoring, induction motors, inverters

## 1. Introduction

Nowadays, induction motors are, and will remain in the future, the most important and frequently used electromechanical machines at industry facilities, but they are also of high interest in academic studies [1]. These machines are very important and are used because of their overall benefits, such as low cost, relatively easy manufacturing, robustness in performance, reliability, wide range of power capacities, and easy maintenance [2]. These motors represent around 80% of the used equipment and around 60% of the total energy consumption in the industry [3, 4]. Normally, electric motors are used with other elements such as mechanical couplings, drivers, and power sources to properly operate and to provide motion in the process [5].

The typical applications can be observed as domestic like in drills, pumps, blowers, vacuums, etc. or as industrial like in conveyors, machine tools, elevators, etc., which is the industrial application that is of main interest in this work [6]. However, the industrial environments are frequently changing and involve hard conditions related to electrical, mechanical, and thermal situations, among others, that directly or indirectly induce stresses to the induction motor [7]. These stresses cause malfunctioning, faults, or wear in many mechanical parts of the motor such as bearings, shafts, rotor bars, as well as in the electrical parts like in the stator and rotor windings [8]. The final consequences of these problems are observed as process downtimes during the motor operation and economic losses, which could be avoided through a correct monitoring and diagnosing process [9]. Thus, the importance of analyzing induction motors and their peripheral elements is justified because of their importance in the industry and domestic applications.

Regarding the importance of the induction motor, many works have been proposed with the purpose to develop methodologies capable of performing the monitoring and diagnosis of this industrial machine. For example, the work developed in [10] presents a methodology based on the motor current normalized residual harmonic analysis (MCNRHA) for diagnosing the rotor faults of broken bars and inter-turn short circuits in the stator windings. The residual harmonics are measured by means of the linear fast Fourier transform spectrum (LFFTS) of the healthy motor current signal and the faulty condition. In another example, the research presented in [11] calculates a fault intensity index in induction motors for the inter-turn short circuit fault of the stator winding. For this purpose, the raw current signal in the time domain obtained from the motor is processed through the discrete wavelet transform (DWT), and by using the detailed coefficients, the statistical parameter of the maximum norm is computed under several load conditions and fault severities. A common approach for detecting faults in the induction motor is based on the motor current signature analysis (MCSA); for instance, the work described in [12] presents an approach for detecting the misalignment fault. But that work uses the load torque signature analysis (LTSA) for studying a mechanism that transmits power between the motor and the loads by using different types of couplings. The obtained results show that these techniques perform according to the particular coupling defined. An interesting methodology for diagnosing the half-broken rotor bar (BRB) fault in an induction motor drive is developed in [13]. In that work, the motor was running under different operation conditions using a variable frequency drive (VFD), and the square of the current signal is analyzed because it generates more fault frequency components. To perform the diagnosis, the multiple signal classification (MUSIC) is implemented in an algorithm that can generate a pseudo-spectrum of the current signal. On one hand, the investigation developed by [14] presents an algorithm based on the Kalman filter (KF) for the stator inter-turn fault detection of induction motors. Thus, the KF is applied to extract the motor current signatures and motor voltage signatures; these signatures are later used for determining statistical fault indexes based on the standard deviation. A particular characteristic of the algorithm is that the effect of harmonic pollution is also analyzed, demonstrating to be effective in such conditions. As an alternative to the classical signal-based approaches such as voltages and currents, some other sensor signals have been considered for the monitoring and analysis of induction motors. For example, thermal image processing has been proposed, such as in [15], where three-phase induction motors are analyzed for fault detection. In this case, the thermal images are converted into a new color model for identification known as hue saturation and value (HSV), and then, five

image segmentation methods are applied for obtaining the hue region: Sobel, Prewitt, Roberts, Canny, and Otsu. Next, different statistical parameters are obtained from the image matrices segmented for detecting three fault conditions under different load conditions: outer race bearing fault, inner race bearing fault, and ball bearing defects. On the other hand, the sound, acoustic, and vibration signals have also been addressed for analyzing induction motors and detecting faults. The case of acoustic signals is handled in [8], where the shortened method of multi-expanded frequency selection was developed together with the K-nearest neighbor (KNN) classifier. Meanwhile, the sound and vibration signals are adopted in the work reported in [16], by implementing the complete ensemble empirical mode decomposition (CEEMD) that divides the analyzed signals into intrinsic mode functions. Posteriorly, the frequency of the marginal Gabor representation is computed with the purpose of obtaining the spectral content in the frequency domain. The method was validated for two broken rotor bars. In summary, the several works discussed demonstrate that several methodologies through classical techniques have been reported, but not all the potential problems associated with induction motors have been addressed. For instance, many of the fault diagnostics are focused on the main elements of the motor, but other peripheral elements are not completely analyzed yet, such as those related to renewable energy systems.

In relation to renewable energy systems used for feeding through inverters and motor drives, some works have addressed this topic. An example of the renewable energy systems used for feeding induction motors is described in [17]. In such work, a system that supplies power energy through photovoltaic panels instead of a bank of batteries is presented. The proposed system integrates solar panels, a push-pull converter, and a pump (induction motor). The objective was to design a system by using the evaluation of the energy-processing cycles allowing optimizing a sensorless induction motor drive. In another case, a similar application was handled in the research reported by [18] that developed a simplified system for water pumping by using an induction motor and photovoltaic panels. This system considered two stages, the first being the extraction of the maximum power from the solar panel through the control of the duty ratio in a DC-DC boost converter using the maximum power point tracking (MPPT) technique. In the second stage, a source inverter operates the pump based on a scalar-controlled voltage way. However, the system was tested under different load conditions in a laboratory-controlled environment. On one hand, some works have focused on the motor feeding through the power inverter such as in [19]. That work has explored the topology of a power inverter type Z-source series for feeding an induction motor by using photovoltaic panels, considering that the inverter has a single-stage conversion with buck-boost capability. Additionally, from this study, it was concluded that the system has benefits such as current and harmonics reduction compared with a simple boost control scheme. In the same line, other works like the research presented by [20] developed a fuzzy logic controller for improving the speed response, reducing harmonic content, and enhancing the overall system performance of a multi-level power inverter used for feeding an induction motor. The proposed system integrates a photovoltaic panel, a boost converter, a multi-level inverter, a classical proportional-integral (PI) controller, and a three-phase induction machine; however, the performance of the approach is verified through simulations in MATLAB and Simulink. Finally, in [21], a power system based on auxiliary photovoltaic panels for electric vehicle applications is presented. The system novelty is a foldable scissor mechanism enabling the power system portability. Like the previous works, the validation of the system was carried out utilizing simulation experiments.

As observed from the previously discussed works, the effects of applying systems for supplying induction motors through devices based on renewable energy such as solar photovoltaic imply the use of power inverters. The effects of these inverters have been addressed from the system improvement viewpoint, considering, for example, hardware topologies. However, the effects of the power inverters considering the type of source output have not been completely analyzed yet and represent an area of opportunity.

In this chapter, the effects caused by the power inverters integrated in a renewable energy generation system, in islanding mode, over induction motors are analyzed. The analyzed system considers the connection of photovoltaic panels to two types of power inverters that are interchanged between the experimental tests. The connected inverter will supply an induction machine and a bank of batteries for power storing. Some physical magnitudes that consider electrical signals (current and voltage), vibration signals, and the motor speed will be acquired through a data acquisition system (DAS), for the behavior analysis. The power inverters considered are categorized into two main types: modified sine wave and pure sine wave. The main differences between the two devices are the internal hardware structures and topologies to generate the sine wave that will be used for supplying the motor. Additionally, the analysis of the inverters' effects will be done under different load conditions. Therefore, some metrics such as ranges, rms values, and harmonic distortion, obtained from the measured signals, will be presented and discussed, demonstrating the differences when the two types of power inverters feed the induction motor. Finally, the experimental results demonstrate how the motor operation varies depending on the type of power inverter by presenting noticeable variations in the percentage of the metrics when modified sine wave is used instead of pure sine wave.

## **2. Theoretical background**

Next, the theoretical background of the power electronics used by solar photovoltaic generation systems (SPVGS), and even by some wind power generation systems (WPGS), will be addressed. The addressed theory focus particularly on the technologies that take the produced alternating current energy and convert it into direct current energy, better known as power inverters.

### **2.1 Power inverter**

Nowadays, among all the types of renewable energy generation systems, solar PV technologies are the most frequently used for power generation because of the merits of the solar energy source, like its abundance (it is found practically in any place around the globe), less maintenance, no rotating or mechanical parts, low operational costs, and being pollution free. Thus, due to all these advantages, the SPVGS have more research and technological developments for all their integrated parts. In this sense, in the renewable energy generation systems, mainly in the SPVGS, it is very common to use power electronic components for providing an adequate energy output, for instance, through the power inverter. Essentially, the generation systems of renewable energy (GSRE) produce the output, in many cases, as direct current (DC) electricity, such as in the case of solar photovoltaic (SPV) systems. Additionally, this energy produced by the GSRE can be also stored in battery banks in the DC form due to several considerations, such as excess power generation, backup power, and

limitations of the generation system. Such limitations in the energy generation process assume that the stored energy can be provided to the final user through the battery banks, as a stable DC power source, when the GSRE is unable to generate power energy, like at night for the case of SPVGS or lack of wind for the case of WPGS. Later, this DC output needs to be converted into alternating current (AC), which is because the loads used in domestic and business applications normally require the signal source in this AC form [22]. Therefore, a power inverter is a device that takes the generated power in the form of DC from the GSRE, or takes the energy stored in the battery bank, and turns it into AC power to operate the final loads [23]. Thus, the power inverter is a key device that normally comes together with the photovoltaic panels strictly used for obtaining an AC source.

It must be mentioned that due to the tendency of reduction in the prices for solar PV systems, it has caused an increment in the research about power inverters addressing considerations such as efficiency, size, weight, reliability. Therefore, today, the power inverter research industry has grown significantly and has developed a wide variety of inverter topologies with the purpose to meet the requirements of power conditioning. For example, Ref. [24] has presented a general classification of the existing inverters considering aspects such as the number of processing stages, the type of isolation, the power rating, the output shape, the voltage gain, the type of grid interface, and the soft/hard switching. Many of these topologies consider the signal output in the form of a pure sine wave, or a modified sine wave, with the main difference in the final applications. The topologies that use pure sine wave signal output are mainly designed for on-grid connections, meaning that the produced energy from the GSRE needs a signal capable of being synchronized and integrated into the commercial grid. In the other case, in many commercial, domestic, and a few cases of business applications where an off-grid connection will be used, better known as islanding appliances, a power inverter topology with modified sine wave signal output will be considered.

It is worth mentioning that although the power inverter is an important device, it can pollute the power signal, mainly affecting its quality by producing power disturbances (PD) such as spikes and harmonic content. This poor power quality (PQ) affects the final equipment fed by the power energy from the inverter and is reflected as losses and delivered heat, causing malfunctioning and even damage [24]. Therefore, the effects and impacts of the power inverters are a topic of interest because they are not fully addressed yet for application where induction motors are fed through renewable energy systems.

### 3. Experimental setup

The experimental test bench used for the validation of this proposal consists of a photovoltaic system that is used as a renewable energy generation system; the photovoltaic system is connected in an isolated way, and it is used to provide the power supply to a single-phase induction motor (IM); the general wiring of the aforementioned photovoltaic system is represented in **Figure 1**. As noted, the renewable energy generation system is composed of three solar cells (model SL150TU-18P), producing an average peak power of around 150 W per cell; a solar charge controller (model NV12V010E) is also taken into account since it is responsible for regulating the state-of-charge of a set of batteries (three batteries with model CL-31 T-700). Thus, the set of batteries allows to store the energy produced by the photovoltaic system

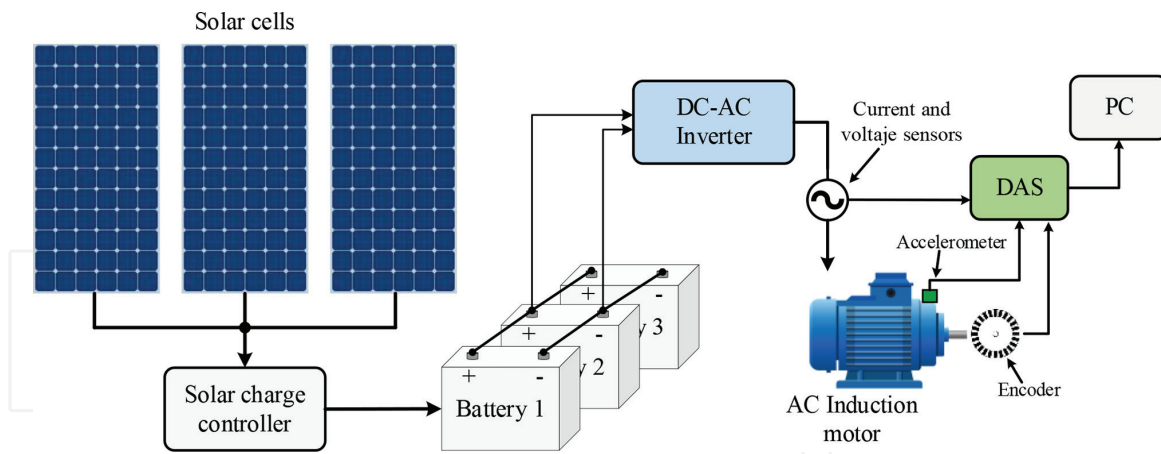


**Figure 1.** General flowchart representing the wiring of the photovoltaic renewable energy generation system and the instrumentation to monitor several physical magnitudes.

(DC voltage), and then, the stored energy is converted into AC voltage by means of a DC-AC inverter. In this regard, it must be clarified that two different inverters are used for transforming the energy from DC to AC; one of the inverters is a 1500 W pure sine wave inverter (model RBP1500WRD by WZRELB), whereas the other one is a 1500 W modified sine wave inverter (INCO-1500 by TRUPER). The main technical characteristics of the two inverters are summarized in **Table 1**.

From **Table 1**, it is observed that both power inverters have similar characteristics; however, it is worth mentioning that the pure sine wave inverter is designed to limit the amount of harmonic components that can be found in the output signal. In this particular case, the THD value always remains under 5%, a situation that indicates that the resulting voltage signal is accomplished with international power quality standards. On the other hand, the modified sine wave inverter does not provide information regarding the THD. Nonetheless, this type of inverter is characterized by delivering a nearly squared signal; that is, the amount of harmonics is expected to be high. In fact, this last issue is one of the motivations for developing this study to find the repercussion of feeding an induction motor with a voltage signal that contains a high amount of harmonics and interharmonics.

Specification	Pure sine wave inverter	Modified sine wave inverter
Model	RBP1500WRD	INCO-1500
Manufacturer	WZRELB	TRUPER
Rated power	1500 W	1500 W
DC input voltage	10–15 V	10.5–15.5 V
AC output voltage	110 V	120 V
Frequency	60 Hz	60 Hz
Maximum efficiency	90%	85%
Total harmonic distortion (THD)	< 5%	Not provided by manufacturer

**Table 1.** Technical characteristics for the DC-AC inverters used in the experimentation.

As stated, the use of these inverters is to analyze the effects that are produced over a 372 W single-phase IM (model 1RF20000DB004AB1 by SIEMENS) with two pairs of poles, efficiency around 62%, nominal rotating speed of 1755 RPM, and a nominal stator current consumption of 5.6 A (rms); the IM is used as the AC load connected to each one of the tested inverters.

Furthermore, for monitoring the operation of the IM, several sensors are installed to measure different physical magnitudes; therefore, a hall-effect current sensor (model SCT-013-030) is installed through the power supply lines to monitor the IM stator current consumption, and a transformer-based sensor (model ZMPT101B) is used to monitor the supply voltage; similarly, a triaxial accelerometer (model LIS3L02AS4) is installed over the IM case in the end-drive shaft in order to acquire the vibrations produced by the rotating movement, and an encoder is also installed in the IM shaft to measure the rotational speed. These sensors are installed and located as illustrated in **Figure 1**. The signals are acquired by means of two 12-bit 4-channel serial-output sampling analog-to-digital converters (ADS7841) that are mounted on a self-designed data acquisition system (DAS), which is based on a field programmable gate array (FPGA) technology. Thus, a sampling frequency of 6000 Hz is programmed in the proprietary DAS to acquire the stator current signal, the voltage signal, and the rotational speed, whereas the vibration signals are acquired with a sampling frequency of 3000 Hz. Accordingly, the aforementioned signals are continuously acquired during 30 seconds that comprise the start-up and the steady state of the IM, where the considered inverters are tested iteratively in order to perform several runs in the IM; all the acquired data are stored in a personal computer for posterior analysis.

#### 4. Proposed methodology

The proposed methodology for analyzing the effects produced by pure sine and modified sine inverters in a single-phase IM consists of three main steps that are summarized in the flowchart of **Figure 2** that consist of *data acquisition*, *data processing*, and *analysis*.

In the *data acquisition* stage, the stator current, voltage, vibrations, and rotational speed are continuously acquired during 30 seconds of the IM operation; these signals are acquired by the proprietary DAS when the IM is fed through the pure sine and modified sine inverters, iteratively. In this regard, several tests are performed with each different inverter with the aim of comparing the repeatability of the experiments.

Subsequently, in the second stage of *data processing*, the acquired signals are subjected to a processing procedure by means of estimating the power spectral density

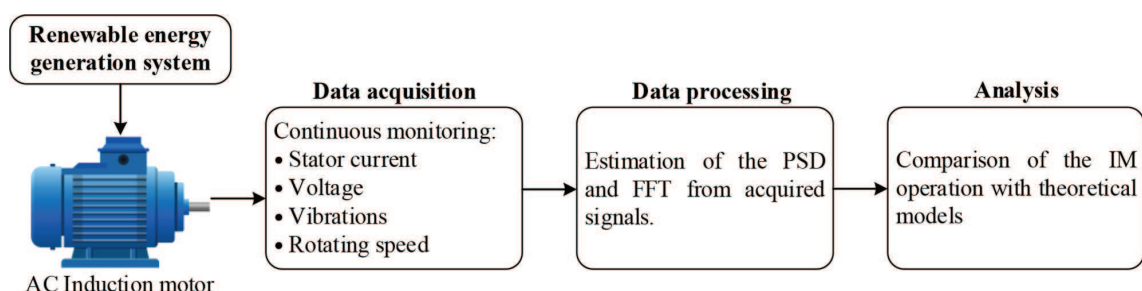


**Figure 2.**  
Proposed methodology for analyzing the effects produced by pure sine and modified sine inverters in a single-phase IM.



(PSD) and by estimating the fast Fourier transform (FFT); precisely, the PSD is performed from the stator current, whereas the FFT is performed from the vibration signals. On the other hand, the raw voltage signal is analyzed in the time domain in order to compare similarities and differences between signals from the pure sine and modified sine inverters. Similarly, for both the inverters, the rotational speed signals are compared between them with an aim to identify the main differences, and such signals are also taken into account for a precise estimation of the theoretical frequencies that characterize the operation of the IM under study.

Finally, in the stage of *analysis*, the previous estimated PSD and FFT locate the theoretical frequencies that characterize the electrical and mechanical operation of the IM; that is, for the electrical signal, a frequency component must be located in  $f_s$  as the supply frequency component, and the mechanical operation is represented by  $f_r$  as the rotational speed; for both frequency components ( $f_s$  and  $f_r$ ), some harmonics may appear according to the IM condition. In this sense, the most common faulty conditions that affect the operation of IMs are misalignment, unbalance, bearing defects, and broken rotor bars; thus, the harmonics of  $f_s$  and  $f_r$  may be more evident depending on whether the IM is working under the influence of any defect or not.

## 5. Results and discussions

The proposed method is performed in order to analyze the effects produced by pure sine and modified sine inverters in a single-phase IM; thus, the IM is fed through two different inverters, iteratively. Therefore, during the experimentation, several signals have been acquired and stored in a personal computer, and each measured signal comprises the start-up to the steady state of the IM; the signals are acquired during 30 seconds.

Accordingly, **Figure 3a** and **b** shows the rotational speed achieved by the IM in its end-drive shaft when the pure sine and modified sine inverters are used to feed such IM; the average speed that is reached during the steady state for each corresponding case is around 1799 rpm and  $1794 \pm 4$  rpm, respectively. Thus, regarding the nominal speed provided by the manufactured IM, a speed variation between 2% and 3% is achieved when the IM is fed through both inverters. As shown in **Figure 3a** and **b**, there are some specific differences that characterize the working operation of the IM; probably, the main difference relies on the time that the IM requires to reach the steady state; precisely, **Figure 3a** depicts a soft start, where the IM achieves the steady state in an average time of around 1.9 seconds, whereas **Figure 3b** depicts an abrupt start, where the IM requires approximately 0.6 seconds to achieve its steady state. Thus, a soft start is preferred since it may lead to producing low stator currents during the start-up and may also benefit to avoid inducing structural damage to the whole elements that are linked to the IM, that is, rigid couplings, shafts, pulley belts, and gears, among others. Another difference that can be noted in **Figure 3a** and **b** is the stability of rotation when the IM has reached its steady state; that is, when the IM is fed by the pure sine inverter, a stable rotational speed is produced in the end-drive shaft (**Figure 3a**), whereas a variational rotating speed is generated when the modified sine inverter is used (**Figure 3b**). Thereby, most of the time, some processes and/or applications are affected when the rotational speed of the IM that drives such processes is variable; that is, an electric water pump may produce a variable flow of water if the rotating speed of impellers is not constant. Moreover, the sudden occurrence

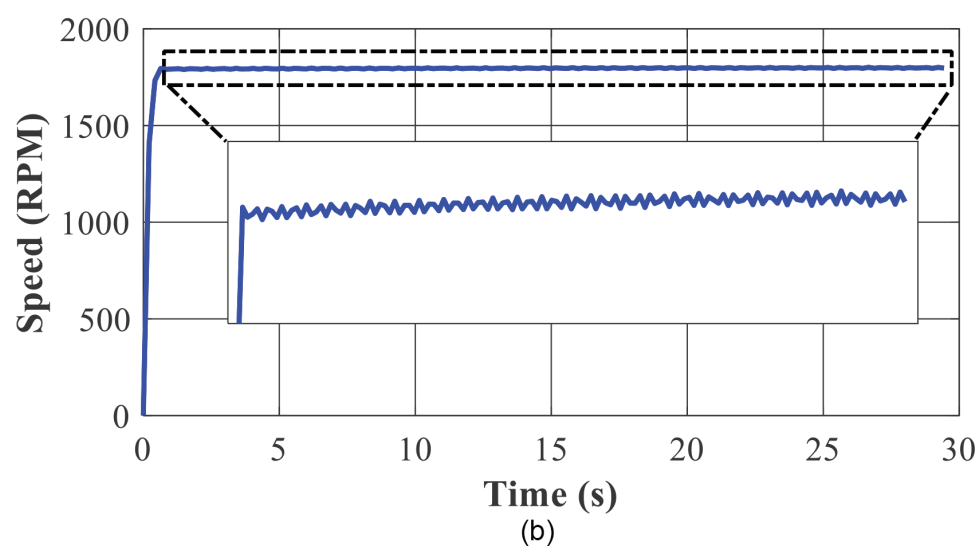
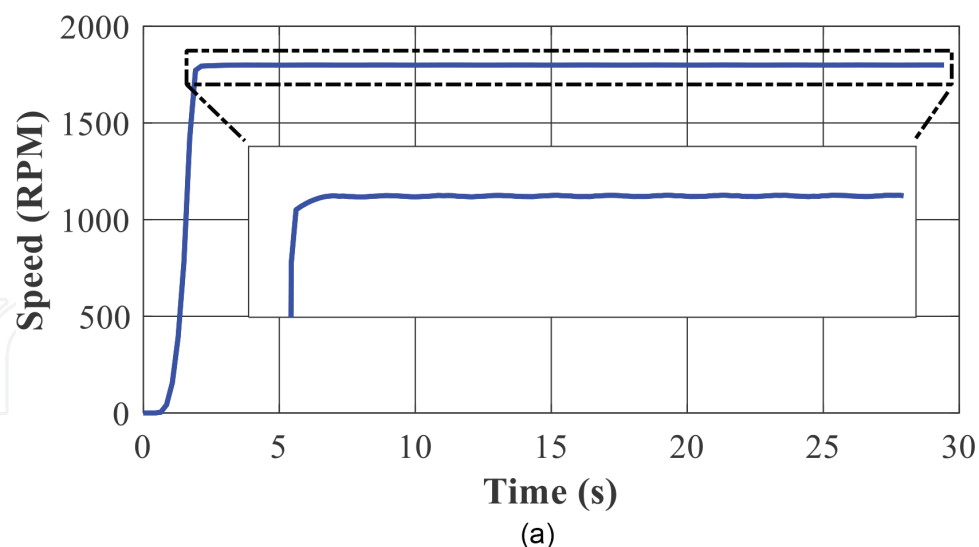
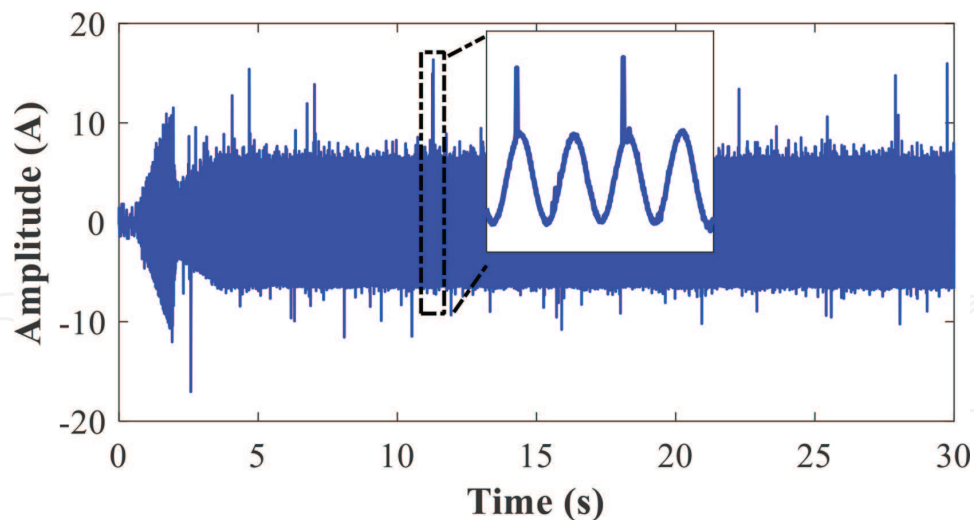


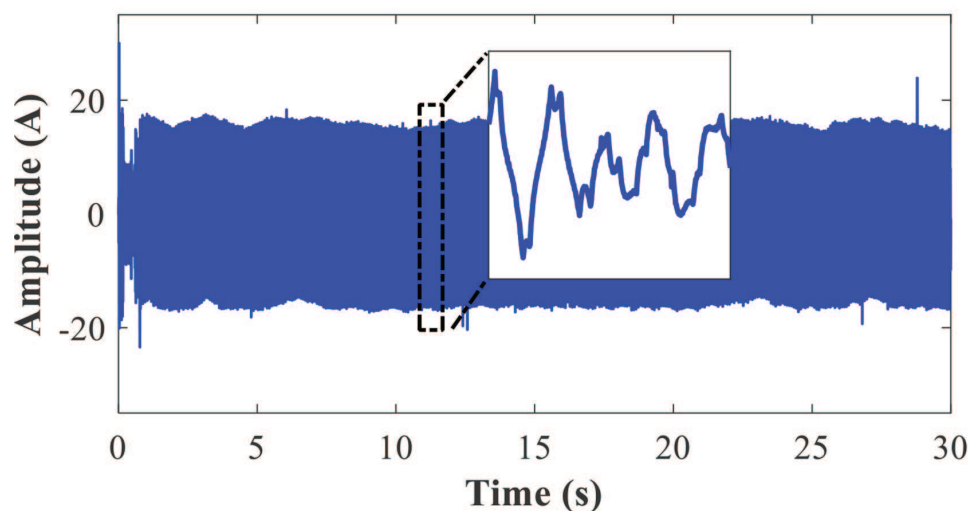
**Figure 3.** Rotational speed achieved in end-drive shaft of the IM when it is fed through a) the pure sine inverter and b) the modified sine inverter.

of vibrations may affect and induce damage over the whole elements linked to the IM that experiences variable speed.

Consequently, **Figure 4a** and **b** shows the measurements of the stator current consumption when the IM was fed through the pure sine and modified sine inverters, respectively. As it can be appreciated, the soft starting produced by the pure sine inverter also leads to a reduced current consumption during the start-up; such current consumption is approximately 11.5 amperes peak. Once the IM has achieved its steady state, the average current consumption is around 6.5 amperes peak, and although **Figure 4a** depicts the stator current in the IM when it is fed with the pure sine inverter, an almost perfect sine wave with some speaks is measured. In this sense, the current signal is dirty since the AC-DC inverter is composed of several power electronic elements. On the other hand, high current consumption is demanded by the IM when it is fed with the modified sine inverter as illustrated in **Figure 4b**, where a peak current consumption higher than 25 amperes is reached and an average current consumption of around 9.4 amperes is produced in the steady state. In addition, the shape of the current wave in **Figure 4b** is not sinusoidal and consumption



(a)

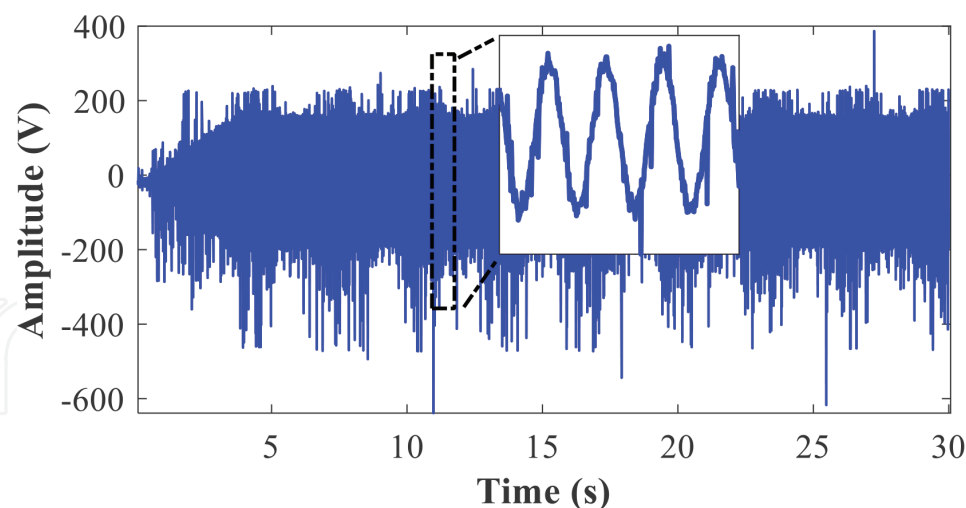


(b)

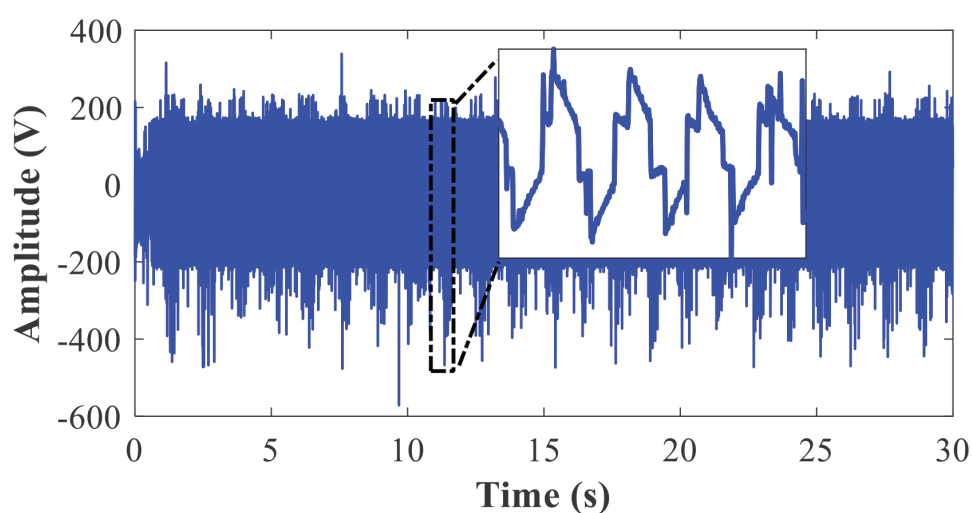
**Figure 4.** Measurements of the stator current consumption produced in the IM when it is fed through a) the pure sine inverter and b) the modified sine inverter.

shows several variations; this fact is due to the power quality characteristics that have the modified sine inverter. Thus, the most critical increase in the stator current consumption is presented during the start-up where the increase is more than 200% by comparing the current peak of **Figure 4a** and **b**; meanwhile, percentages around 82% and 118% are achieved during the steady state in comparison with the nominal current consumption given by the manufacturer.

Voltage signals are shown in **Figure 5a** and **b**, respectively, for each one of the considered inverters, pure sine and modified sine. As it is observed, both voltage signals are generated with a peak amplitude of about 180 volts; also, both signals show distortion that in terms of power quality can be understood as harmonics, sags, swells, and transients, among others. Precisely, in the zoomed-in view shown in **Figure 5a**, a transient is noted, which is also present in the whole voltage signal; on the other hand, the zoomed-in view of **Figure 5b** also shows transients that in general may affect the proper operation of the IM. Hence, all the electronic elements included in both inverters are the main source that leads to producing voltage signals with high distortion.



(a)

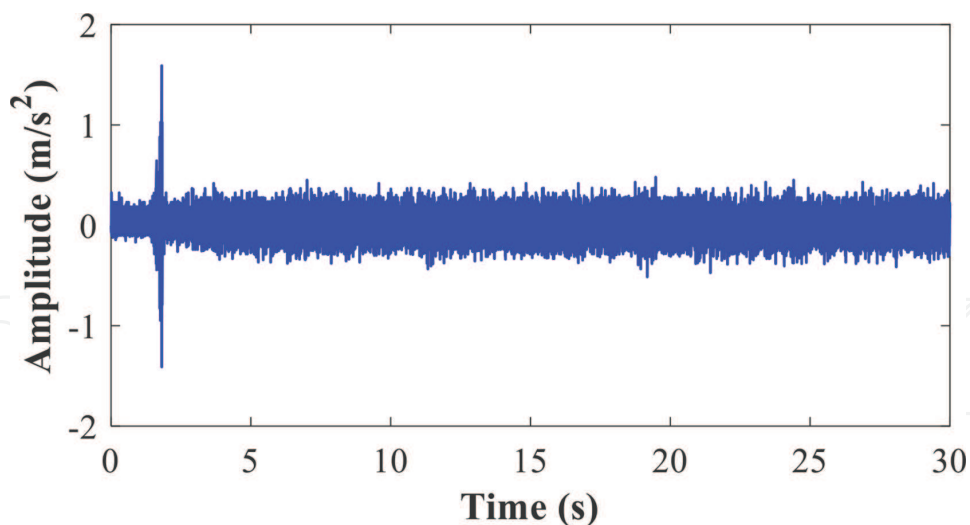


(b)

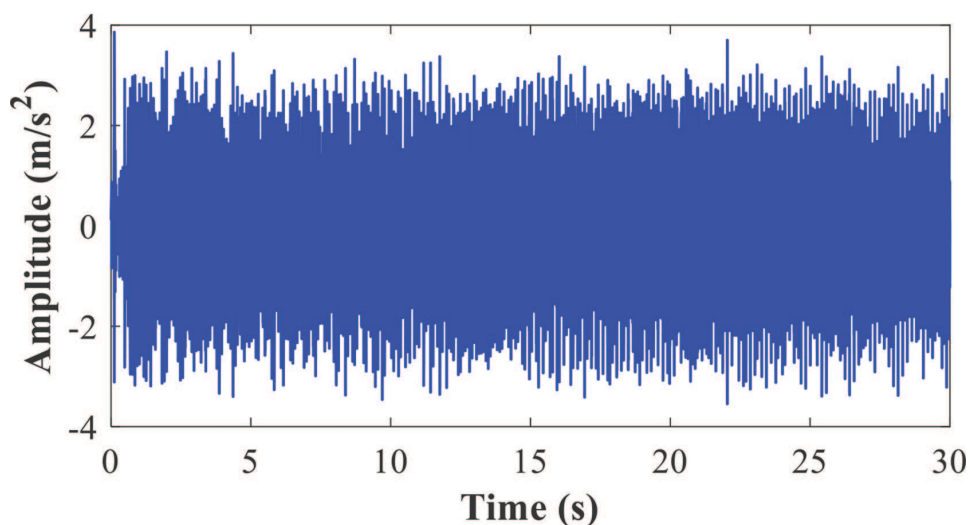
**Figure 5.** Recorder voltage signals produced by the considered AC-DC inverters to feed the IM: a) the pure sine inverter and b) the modified sine inverter.

On the other hand, the main difference between the voltage signals of **Figure 5a** and **b** is the shape, where the voltage signal in **Figure 5a** depicts an almost perfect sine wave, while the voltage signal in **Figure 5b** does not have a sinusoidal wave. In this regard, it must be highlighted that a high harmonic content is inherent in the voltage generation for both inverters. Additionally, the THD is estimated from both acquired signals in order to validate the percentages of distortion given by the manufactures; in this way, distortions of around 5.5% and 22.3% are computed for both inverters, pure sine and modified sine, respectively.

The acquired vibration signals are associated with the mechanical operation of the IM; in fact, any AC rotating machine may experiment with different operating conditions when fed through a renewable power supply by means of inverters. For example, if an AC electric motor is connected to a power supply, the power quality can affect the operation of the device, producing speed variations since it is in function of the voltage applied. Subsequently, the acquired vibrations when the IM is fed through the pure and modified sine inverters are shown in **Figures 6a** and **b**, respectively; as it is observed, the vibrations produced in the



(a)



(b)

**Figure 6.** Acquired vibration signal in the radial axis of the IM when it is fed through both inverters: a) the pure sine inverter and b) the modified sine inverter, respectively.

IM have higher amplitude when it is fed through the modified sine inverter, while the level of vibrations is reduced when the pure sine inverter is used as the power supply source. Also, there are some differences between **Figure 6a** and **b**; that is, a transient vibration spike is presented at the end of the start-up of the IM when it is fed with the pure sine inverter, and then, the vibration level is retained with a specific average amplitude. On the other hand, the IM experiences a high level of vibrations, which apparently is retained during the start-up and the steady state of the IM when the modified sine inverter is used. Qualitatively, by comparing the RMS values of both vibration signals, an increase from 0.0997 to 0.6989 is presented when the IM is fed with sine and modified inverters. For the IM under test, the vibrations are directly produced by the quality of the voltage signal that is provided by both the considered inverters; it should be mentioned that the IM is in a healthy condition; thus, there are no external factors that lead to introducing the occurrence of vibrations. **Table 2** summarizes the most important aspects depicted with the use of pure and modified sine inverters.

Physical magnitude	Pure sine wave inverter	Modified sine wave inverter
Speed	The speed is constant and reaches an average value of around 1799 RPM	The speed shows fluctuations producing an average speed value of $1794 \pm 4$ RPM
Current	The stator current consumption is less than the nominal current consumption	An increase of around 118% of the stator current consumption is reached during the steady state
Voltage	The distortion is around 5.5% as manufacturer depicts	The distortion is higher than 20% as the shape wave does not match the sine wave
Vibration	An averaged RMS vibration value of 0.0997 is achieved with a soft noise	The vibration increases seven times by considering the RMS vibration value 0.6989

**Table 2.**  
 Technical characteristics for the DC-AC inverters used in the experimentation.

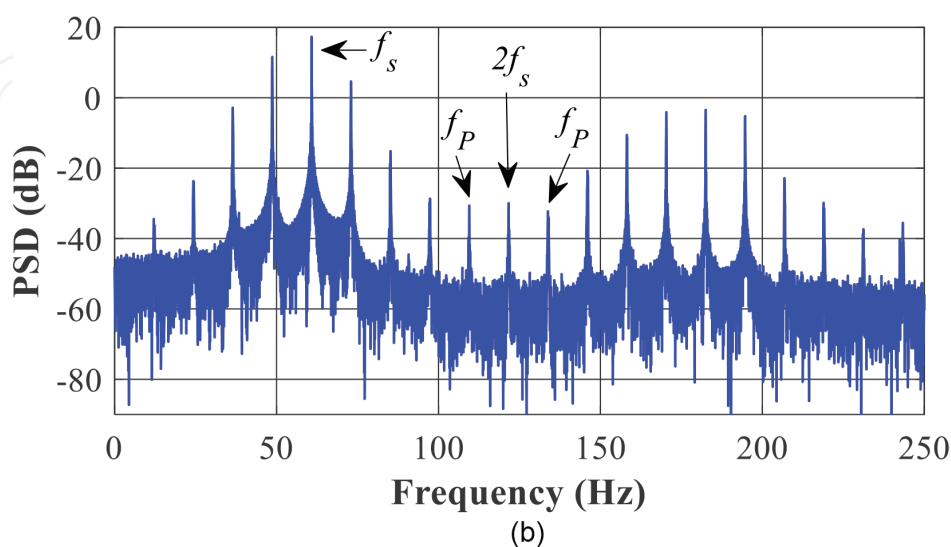
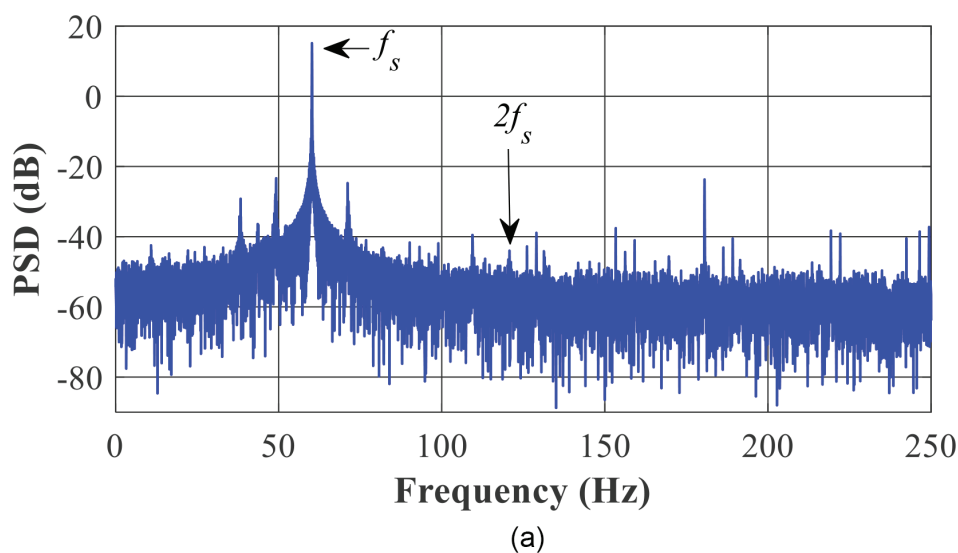


**Figure 7.**  
 Achieved PSD of the acquired stator current when the IM is fed through a) the pure sine inverter and b) the modified sine inverter, respectively.

Accordingly, the PSD of the stator current and the FFT of the vibrations are carried out in order to provide a more accurate analysis of the effects that pure sine and modified sine inverters introduce over the operation of an IM. Therefore, **Figure 7a** and **b** shows the obtained PSD when the pure and modified inverters are used to feed the IM, respectively. Some aspects must be highlighted from these PSDs; the first one is that the supply frequency ( $f_s$ ) is present and it may be located approximately around 60 Hz, and it appears with a high amplitude; the second one is that in the PSD of **Figure 7b** appears a significant number of frequency components with higher amplitude in comparison with the PSD of **Figure 7a**. The appearance of additional frequency components is also due to the quality of the power voltage supply; moreover, as expected, the use of modified sine inverters results in the introduction of frequency components over the PSD that may be masked and/or confused with those characteristic fault-related frequency components that are commonly induced by faults such as misalignments, unbalances, short circuits, and broken rotor bars, among others. Specifically, in the PSD of **Figure 7b** are induced several harmonics related to  $f_s$ ; such harmonics appear at  $2f_s$  and  $3f_s$ , but the  $2f_s$

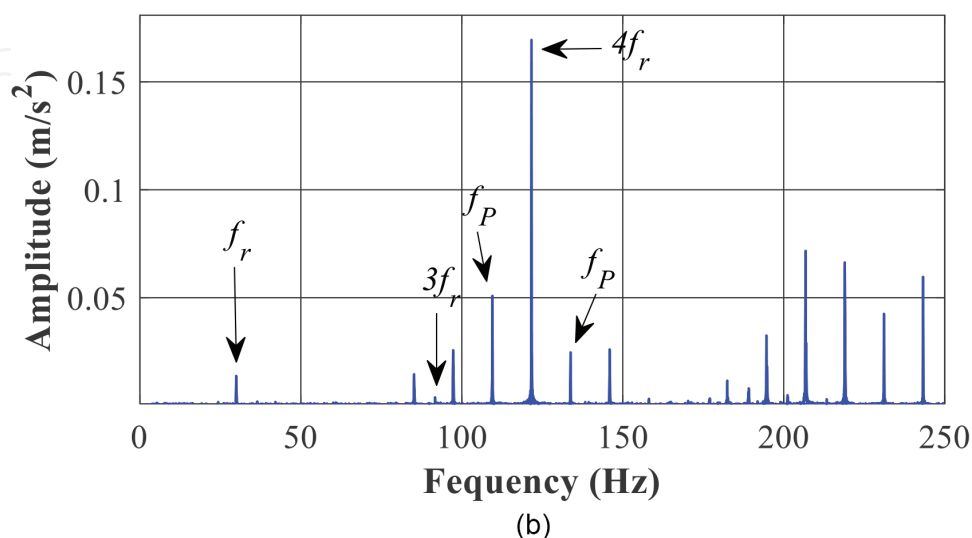
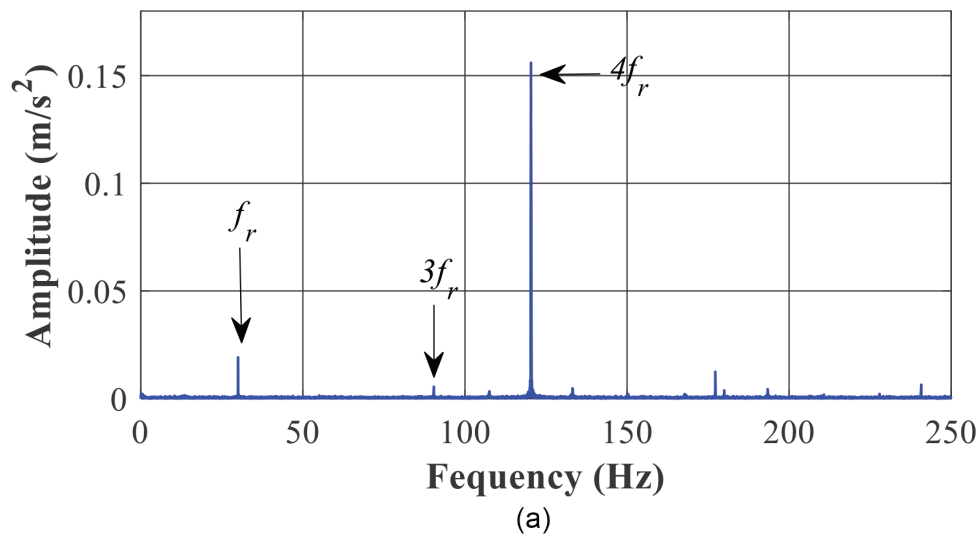


**Figure 8.** Achieved FFT of the acquired vibrations when the IM is fed through a) the pure sine inverter and b) the modified sine inverter, respectively.

components may increase their amplitude when problems associated with phase problems are inherent to the power supply; additionally, sidebands may appear around  $2f_s$  that are associated with the pole pass frequency ( $f_p$ ). Thereby, in **Figure 7b**, a significant increase of frequency components ( $2f_s$  and  $3f_s$ ) as well as the occurrence of additional frequency components ( $f_p$ ) that ideally depict malfunction problems in the power supply is observed.

Finally, the vibration signals are processed by means of estimating the frequency spectra through the FFT; thus, **Figure 8a** and **b** shows the resulting vibration spectra that belong to the IM operation when it is fed with the pure and modified sine inverters, respectively. As it is observed in both spectra, some characteristics related to frequency components appear, where it is important to identify the frequency component associated with rotational speed ( $f_r$ ) that is reached in the IM; also, there are some harmonics of  $f_r$  that can be identified over both spectra such as the third and fourth harmonics ( $3f_r$  and  $4f_r$ ). The aforementioned harmonics are the most important since it is around these frequency components that sideband frequencies appear, separated by the pole pass frequency ( $f_p$ ) when the IM is fed through the modified sine inverter. Thus, the quality of the voltage power supply also affects the mechanical operation of electric rotating machines such as IM even if such machines are in healthy condition; such affectations commonly produce variations in the rotational speed, generation of abnormal noise during the steady state, and sometimes the occurrence of structural vibrations that affect the whole components of the IM. On the other hand, the use of pure sine inverters allows to operate the IM almost as it was working under conventional conditions where the power supply voltage is provided by an electrical factory.

## 6. Conclusions

This work presented an analysis of the effects produced in an IM when it is fed through renewable energy by means of pure sine and modified sine inverters; the analysis consists of acquiring some physical magnitudes such as the stator current that is consumed by the IM, the voltage supplied to the IM, the rotational speed reached in the end-drive shaft of the IM, and the mechanical vibrations produced by the IM during its working operation. These signals are continuously acquired and are first compared in the time domain. Regarding the obtained results, it can be concluded that a slight reduction in the stator current consumption is achieved when the IM is fed through the pure sine inverter; also, a soft start-up is produced, the average rotational speed is retained in the end-drive shaft, as well as vibration levels are kept low. Meanwhile, when the IM is fed through the modified inverter, the stator current consumption increases, and this increase may lead to an increase in the temperature of the IM and several damages can be also produced. Additionally, the modified inverter makes the IM rotate with variations and noise, and subsequently, the occurrences of vibrations are present in the whole IM case. Finally, the stator current and vibrations are also analyzed by means of the PSD and FFT, where significant differences are appreciated by comparing the resulting spectra when the IM is fed with both the considered inverters. The most important aspect to be highlighted from the PSD and FFT is that the modified sine inverter leads to the introduction of a frequency component that is associated with the pole pass frequency, where such a component is associated with phase problems. Finally, pure sine inverters are recommended in



applications where rotating machines are involved; in fact, the consideration of pure sine inverters may result in extending the useful life of those elements that are fed through them as much as possible.

## **Acknowledgements**


This work has been partially supported by the “FONDO PARA EL DESARROLLO DEL CONOCIMIENTO” (FONDEC-UAQ 2022) under the project “Analysis and detection of failures in alternative energy power generation systems through artificial intelligence algorithms and machine learning techniques”.

## **Author details**

Arturo Yosimar Jaen-Cuellar, David Alejandro Elvira-Ortiz,  
Emmanuel Resediz-Ochoa and Juan Jose Saucedo-Dorantes\*  
Engineering Faculty, Autonomous University of Queretaro, San Juan del Rio, Mexico

\*Address all correspondence to: [juan.saucedo@uaq.mx](mailto:juan.saucedo@uaq.mx)

## **IntechOpen**

© 2022 The Author(s). Licensee IntechOpen. This chapter is distributed under the terms of the Creative Commons Attribution License (<http://creativecommons.org/licenses/by/3.0>), which permits unrestricted use, distribution, and reproduction in any medium, provided the original work is properly cited. 

## References

- [1] Zamudio-Ramirez I, Osornio-Rios RA, Antonino-Daviu JA, Razik H. Magnetic flux analysis for the condition monitoring of electric machines: A review. *IEEE Transactions on Industrial Informatics*. 2022;**18**(5):2895-2908
- [2] Corral-Hernandez JA, Antonino-Daviu JA. Thorough validation of a rotor fault diagnosis methodology in laboratory and field soft-started induction motors. *Chinese Journal of Electrical Engineering*. 2018;**4**(3):66-72
- [3] Kumar S, Mukherjee D, Guchhait PK, Banerjee R, Srivastava AK, Vishwakarma DN, et al. A comprehensive review of condition based prognostic maintenance (CBPM) for induction motor. *IEEE Access*. 2019;**7**:90690-90704
- [4] Errigo A, Choi JK, Kissock K. Techno-economic-environmental impacts of industrial energy assessment: Sustainable industrial motor systems of small and medium-sized enterprises. *Sustainable Energy Technologies and Assessments*. 2022;**49**:101694
- [5] Vadi S, Bayindir R, Toplar Y, Colak I. Induction motor control system with a Programmable Logic Controller (PLC) and Profibus communication for industrial plants — An experimental setup. *ISA Transactions*. 2022;**122**:459-471
- [6] Zhang J, Wang P, Gao RX, Sun C, Yan R. Induction motor condition monitoring for sustainable manufacturing. *Procedia Manufacturing*. 2019;**33**:802-809
- [7] Jeffali F, Ouariach A, El Kihel B, Nougauoui A. Diagnosis of three-phase induction motor and the impact on the kinematic chain using non-destructive technique of infrared thermography. *Infrared Physics & Technology*. 2019;**102**:102970
- [8] Glowacz A. Fault diagnosis of single-phase induction motor based on acoustic signals. *Mechanical Systems and Signal Processing*. 2019;**117**:65-80
- [9] Vishwakarma M, Purohit R, Harshlata V, Rajput P. Vibration analysis & condition monitoring for rotating machines: A review. *Materials Today: Proceedings*. 2017;**4**:2659-2664
- [10] Allal A, Khechekhouche A. Diagnosis of induction motor faults using the motor current normalized residual harmonic analysis method. *International Journal of Electrical Power & Energy Systems*. 2022;**141**:108219
- [11] Almounajjed A, Sahoo AK, Kumar MK. Diagnosis of stator fault severity in induction motor based on discrete wavelet analysis. *Measurement*. 2021;**182**:109780
- [12] Verucchi C, Bossio J, Bossio G, Acosta G. Misalignment detection in induction motors with flexible coupling by means of estimated torque analysis and MCSA. *Mechanical Systems and Signal Processing*. 2016;**80**:570-581
- [13] Singh G, Naikan VNA. Detection of half broken rotor bar fault in VFD driven induction motor drive using motor square current MUSIC analysis. *Mechanical Systems and Signal Processing*. 2018;**110**:333-348
- [14] Namdar A, Samet H, Allahbakhshi M, Tajdinian M, Ghanbari T. A robust stator inter-turn fault detection in induction motor utilizing Kalman filter-based algorithm. *Measurement*. 2022;**187**:110181

- [15] Al-Musawi AK, Anayi F, Packianather M. Three-phase induction motor fault detection based on thermal image segmentation. *Infrared Physics & Technology*. 2020;**104**:103140
- [16] Delgado-Arredondo PA, Morinigo-Sotelo D, Osornio-Rios RA, Avina-Cervantes JG, Rostro-Gonzalez H, Romero-Troncoso R. Methodology for fault detection in induction motors via sound and vibration signals. *Mechanical Systems and Signal Processing*. 2017;**83**:568-589
- [17] Vitorino MA, de Rossiter Correa MB, Jacobina CB, Lima AMN. An effective induction motor control for photovoltaic pumping. *IEEE Transactions on Industrial Electronics*. 2011;**58**(4):1162-1170
- [18] Singh B, Sharma U, Kumar S. Standalone photovoltaic water pumping system using induction motor drive with reduced sensors. *IEEE Transactions on Industry Applications*. 2018;**54**(4):3645-3655
- [19] Adle R, Renge M, Muley S, Shobhane P. Photovoltaic based series z-source inverter fed induction motor drive with improved shoot through technique. *Energy Procedia*. 2017;**117**:329-335
- [20] Chandrasekaran S, Durairaj S, Padmavathi S. A Performance evaluation of a fuzzy logic controller-based Photovoltaic-fed multi-level inverter for a three-phase induction motor. *Journal of the Franklin Institute*. 2021;**358**:7394-7412
- [21] Jin Z, Li D, Hao D, Zhang Z, Guo L, Wu X, et al. A portable, auxiliary photovoltaic power system for electric vehicles based on a foldable scissors mechanism. *Energy and Built Environment*. 2022;**2022**:10
- [22] Gorjian S, Shukla A, editores. *Photovoltaic Solar Energy Conversion: Technologies, Applications and Environmental Impacts*. 1st ed. Cambridge: Elsevier; 2020
- [23] Mayfield R. *Photovoltaic Design & Installation for Dummies*. Hoboken, NJ: Wiley; 2010. p. 366
- [24] Dogga R, Pathak MK. Recent trends in solar PV inverter topologies. *Solar Energy*. 2019;**183**:57-73